

 Open access • Proceedings Article • DOI:10.1117/12.616603

## Absolute timing with the SWIFT X-ray telescope (XRT) — Source link

Giancarlo Cusumano, V. Mangano, Teresa Mineo, V. La Parola ...+23 more authors

**Institutions:** INAF, University of Milano-Bicocca, Pennsylvania State University, Goddard Space Flight Center ...+1 more institutions

**Published on:** 18 Aug 2005 - Proceedings of SPIE (International Society for Optics and Photonics)

**Topics:** X-ray telescope

Related papers:

- [In-flight calibration of the SWIFT XRT effective area](#)
- [Swift XRT effective area measured at the Panter end-to-end tests](#)
- [In-flight calibration of the Swift XRT point spread function](#)
- [The Swift X-Ray Telescope](#)
- [The unique observing capabilities of the Swift x-ray telescope](#)

Share this paper:    

View more about this paper here: <https://typeset.io/papers/absolute-timing-with-the-swift-x-ray-telescope-xrt-433efkbcx>

# Absolute timing with the SWIFT X-ray telescope (XRT)

G. Cusumano<sup>a</sup>, V. Mangano<sup>a</sup>, T. Mineo<sup>a</sup>, V. La Parola<sup>a</sup>, A. La Barbera<sup>a</sup>, S. Campana<sup>b</sup>, G. Chincarini<sup>c</sup>, G. Tagliaferri<sup>b</sup>, A. Moretti<sup>b</sup>, P. Romano<sup>b</sup>, M. Capalbi<sup>d</sup>, M. Perri<sup>d</sup>, P. Giommi<sup>d</sup>, D. Burrows<sup>e</sup>, D. Morris<sup>e</sup>, J.E. Hill<sup>e</sup>, J. Kennea<sup>e</sup>, J.A. Nousek<sup>e</sup>, C. Pagani<sup>b,e</sup>, L. Angelini<sup>f</sup>, J.P. Osborne<sup>g</sup>, A.F. Abbey<sup>g</sup>, A. Beardmore<sup>g</sup>, M.R. Goad<sup>g</sup>, K. Page<sup>g</sup>, A. Wells<sup>g</sup>

<sup>a</sup>INAF-IASF Sezione di Palermo, via Ugo La Malfa 153, 90146 Palermo, Italy;

<sup>b</sup>INAF-Osservatorio Astronomico di Brera, via E. Bianchi 46, 23807 Merate (Lc), Italy;

<sup>c</sup>Università degli Studi di Milano Bicocca, Piazza dell'Ateneo Nuovo 1, 20126 Milano Italy;

<sup>d</sup>ASI Science Data Center, via Galileo Galilei, 00044 Frascati, Italy

<sup>e</sup> Dept. of Astronomy & Astrophysics, Penn State University 525 Davey Lab, University Park, PA 16802 USA

<sup>f</sup>NASA Goddard Space Flight Center, Greenbelt, Maryland 20771 USA

<sup>g</sup>Department of Physics and Astronomy, University of Leicester, Leicester LE1 7RH, UK

## ABSTRACT

The X-ray telescope (XRT) on board Swift, launched on 2004 Nov 20, is performing astrometric, spectroscopic and photometric observations of the X-ray emission from Gamma-ray burst afterglows in the energy band 0.2-10 keV. In this paper, we describe the results of the in-flight calibration relative to the XRT timing resolution and absolute timing capabilities. The timing calibration has been performed comparing the main pulse phases of the Crab profile obtained from several XRT observations in Low Rate Photodiode and Windowed Timing mode with those from contemporaneous RXTE observations. The XRT absolute timing is well reproduced with an accuracy of 200  $\mu$ s for the Low Rate Photodiode and 300  $\mu$ s for the Windowed Timing mode.

**Keywords:** Swift, XRT, timing accuracy

## 1. INTRODUCTION

The Swift Gamma-ray burst explorer,<sup>1</sup> launched on 2004 Nov 20, is designed to detect and localize GRBs and to provide autonomous rapid-response observation and long-term monitoring of their afterglow emission in the X-ray and UV/optical band. The observatory incorporates three primary instruments: the Burst Alert Telescope (BAT<sup>2</sup>), the X-ray telescope (XRT<sup>3</sup>) and the Ultra-Violet/Optical Telescope (UVOT<sup>4</sup>).

The XRT main goal is to measure the positions, fluxes, spectra and light curves of GRB afterglows over a wide dynamical range of fluxes. It studies the GRB counterparts starting about 70 s after the BAT discovery and provides GRB positioning with 5 arcsec accuracy within 10 seconds of target acquisition. The XRT is a focusing X-ray telescope operating in the 0.2-10 keV energy band provided with grazing incidence Wolter I mirrors, originally built for the JET-X telescope.<sup>5,6</sup> The XRT focus X-rays onto a single E2V CCD-22 detector at the focal plane, similar to the EPIC MOS flown on XMM-Newton mission.<sup>7</sup> The focal plane detector covers a Field of View of 23 arcmin diameter and is equipped with four calibration sources located at each corner of the detector. The telescope is characterized by a Point Spread Function (PSF) with 18 arcsec and 22 arcsec half power diameter at 1.5 keV and 8.1 keV, respectively.<sup>8</sup> The XRT effective area is  $\sim 135$  cm<sup>2</sup> at 1.5 keV and decreases to  $\sim 70$  cm<sup>2</sup> at 8.1 keV.<sup>9</sup>

The XRT detector supports four readout modes to cover the dynamical range of fluxes and rapid variability expected from GRB afterglows. The transition between modes is automatically performed on board (see<sup>10</sup> for an exhaustive description).

---

Send correspondence to G.Cusumano

G. Cusumano: E-mail: giancarlo.cusumano@pa.iasf.cnr.it, Telephone: +39 091 6809479

The Imaging mode (IM) works at the very beginning of the afterglow observation and it gives the prompt image of the field of view to provide a rapid evaluation of the coordinates of the GRB X-ray counterpart. The CCD operates collecting the accumulated charge on the detector without any X-ray event recognition. The image is highly piled-up and produces no spectroscopy or time resolved data.

The Photodiode mode (PD), designed for very bright sources and for high timing resolution, alternately performs one serial clock shift and one parallel clock shift and the results is a very rapid clocking of each pixel across any given point on the CCD. In this mode, data are telemetered in two different ways: Low Rate (LRPD) and Piled-up (PUPD). In the LRPD mode only pixels above the lower level discriminator threshold are sent down, whereas in the PUPD mode all pixels are sent to ground. Photodiode mode then does not have any spatial information but does produce a spectrum and a light curve with the high time resolution of 0.14 ms. This mode is useful for fluxes up to 60 Crab, however for sources brighter than 3 Crab pile-up is significant.

Windowed Timing (WT) mode is obtained compressing 10 rows into a single one, and reading out only the central 200 columns of the CCD. It therefore covers the central 8 arcmin of the field of view and provides one dimensional imaging. The time resolution of this mode is 1.8 ms and it is useful for fluxes between 1 and 600 mCrab.

Finally, Photon Counting (PC) mode retains full imaging and spectroscopic resolution but with limited time resolution. A full field of view is accumulated every 2.5 sec and the CCD operates in what is known as 'frame-transfer' configuration. This operation mode is suitable for source fluxes below 1 mCrab.

In this paper, we describe the in-flight calibration of the timing resolution and absolute timing capabilities of Swift-XRT LRPD and WT modes. The calibration is performed comparing the absolute phase of the main pulse of the Crab profile with the values obtained from contemporaneous observations performed by RXTE-PCA<sup>11</sup> whose absolute timing has an accuracy of  $2 \mu\text{s}$ .<sup>12</sup> The eight year monitoring of the main pulse phase of the Crab pulsar with the RXTE showed that it is leading the radio main pulse by  $344 \pm 40 \mu\text{s}$  ( $0.0102 \pm 0.0012$  in phase).<sup>12</sup> We then expect that XRT observations and the RXTE contemporaneous ones show this phase shift respect to the zero radio phase.

## 2. OBSERVATION AND DATA REDUCTION

Crab observations were performed for many different off-axis angles and different detector coordinates. A log of the observations used in the analysis is given in Table 1.

The time tag for each pixel of the XRT CCD in LRPD and WT modes requires the knowledge of the source location on the CCD because it assumes that the field of view is dominated by a single bright source and that every photon arrives on the CCD at the source position.

XRT data were first processed by the Swift Data Center at NASA/GSFC to produce calibrated event lists (level 1 data products). They were then filtered and screened using the XRTDAS (v.1.2) software package to produce cleaned photon list files. The total exposures after the cleaning procedure are listed in Table 1 together with the off-axis angles and the source positions in detector coordinates. Moreover, WT data were extracted in a rectangular region 40 pixels wide along the image strip centered on the source; this region includes about 98% of the PSF.

Contemporaneous RXTE observations used for the comparison with XRT results are also listed in Table 1 together with their exposures and off-axis angles. Data were collected in Event Encoded Mode (EEM) that has a time resolution of  $250 \mu\text{s}$  and reduced using the RXTE standard analysis. In particular bitmask-filtered events were produced by using the FTOOL *fselect*. In addition to the usual GTI, a supplementary time filter was applied to the data excluding time intervals with the Earth elevation angles larger than 10 degrees and with a value of the OFFSET less than 0.02 to cut the slews; time intervals with 3 PCUs on were considered. Light curves with the minimum bin size of  $250 \mu\text{s}$  were obtained.

## 3. TIMING ANALYSIS AND RESULTS

XRT and RXTE arrival times were reported to the Solar System Barycentre using the Crab coordinates  $\alpha_{2000} = 05^{\text{h}} 34^{\text{m}} 31^{\text{s}}.97$   $\delta_{2000} = 22^{\circ} 00' 52''.1$  the DE200 reference frame and the barycentric codes included in the reduction software packages (*barycorr* for XRT and *fbary* for RXTE). Data were folded by

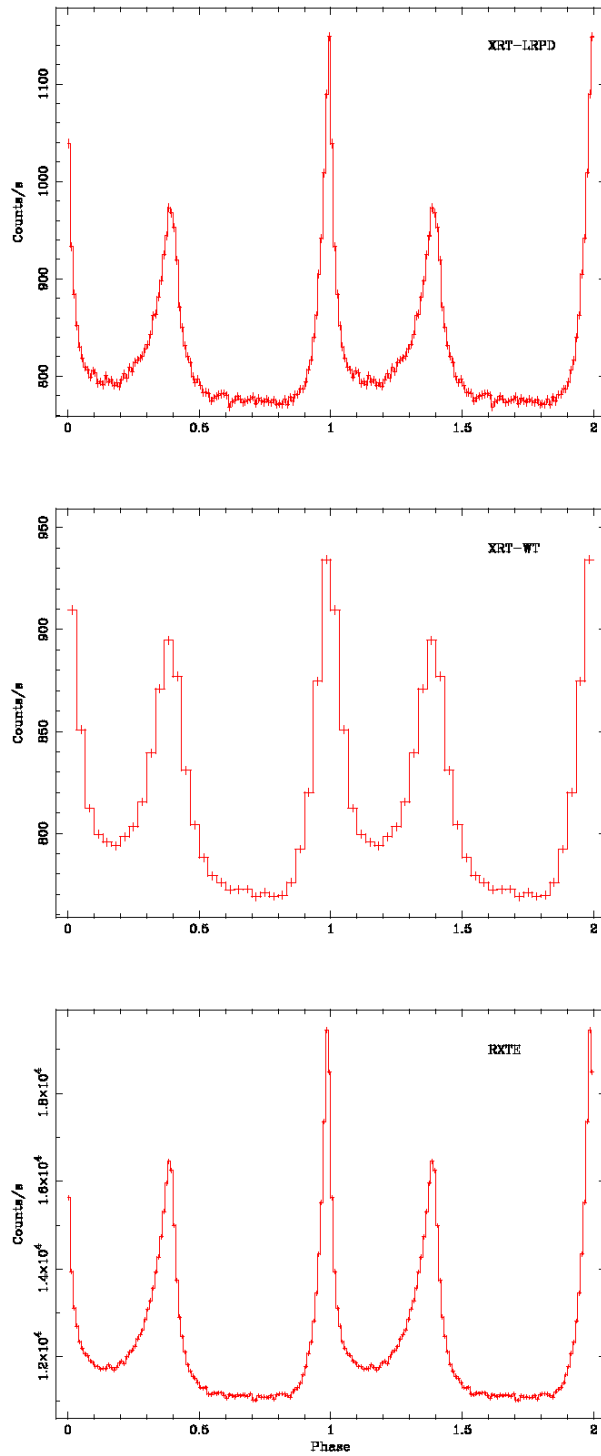


**Figure 1.** Crab pulse profile relative to one LRPD and one WT observation are plotted in the top and middle panel, respectively. The bottom panel shows, for comparison, the light curve from the longest contemporaneous RXTE observation.

**Table 1.** Crab Observation Log

OBS ID	START TIME	MODE	EXPOSURE(s)	OFF-AXIS(°)	DETX	DETY
Swift XRT						
sw00050100008	2004-12-16 14:45:59	LRPD	30.4	0.05	294	305
sw00050100001	2004-12-17 17:47:38	LRPD	652.7	3.6	247	384
sw00050100011	2004-12-30 14:49:00	WT	867.5	2.15	334	338
sw00050100012	2004-12-30 15:08:00	WT	234.5	0.01	295	301
sw00050100007	2005-01-25 00:00:00	WT	4616.8	2.25	336	337
sw00050100010	2005-01-26 00:16:00	LRPD	18432.9	1.96	349	346
sw00050100014	2005-01-29 00:11:51	LRPD	6742.0	1.8	277	317
sw00050101001	2005-02-13 01:20:13	LRPD	58.0	4.8	277	420
sw00050101002	2005-02-13 01:57:01	LRPD	768.3	2.9	306	374
sw00050101003	2005-02-25 14:30:19	LRPD	732.4	3.8	246	380
sw00050102001	2005-02-13 02:56:33	LRPD	115.7	7.6	288	493
sw00050102002	2005-02-13 03:35:01	LRPD	710.5	5.9	311	449
sw00050100016	2005-03-25 00:00:00	WT	7872.2	1.1	294	274
RXTE PCA						
90802-02-11-00	2004-12-03 17:20:00	EEM	709	0.031	–	–
90802-02-12-00	2004-12-17 17:52:31	EEM	1030	0.031	–	–
90802-02-15-00	2005-01-28 11:51:28	EEM	938	0.031	–	–
91802-02-16-00	2005-02-13 01:52:41	EEM	915	0.031	–	–
90802-02-17-00	2005-02-25 14:29:07	EEM	933	0.031	–	–

using the ephemeris provided by the Jodrell Bank radio telescope (UK) that monitors the pulsar monthly (<http://www.jb.man.ac.uk/pulsar/crab.html>). Some of the resulting Crab profiles in absolute phase (the main radio pulse is at phase 0.0) are shown in Fig. 1. In particular, the top and middle panels of Fig. 1 show the folded light curves of sw0005100014 for the LRPD and sw005100016 for the WT mode with time resolutions (0.33 ms for LRPD and 1.1 ms for WT) suitable to the intrinsic time resolution of the two modes. The well known double peaked structure is prominent in the two profiles with very high statistical significance. For comparison, the bottom panel of Fig. 1 shows the profile obtained with the longest RXTE observation (90802-02-12-00) in the energy range 2-15 keV. The shape of the Crab X-ray pulse profiles as measured by XRT in different readout modes and that from RXTE are fully consistent.

In order to determine the phase of the maximum, the central part of the main pulse was fitted with three different models to avoid the systematics that depend on the choice of the fitting function, since the Crab pulse is asymmetric: a Lorentzian, a Gaussian and a parabola. All models give consistent values of the peak phase. In the top and in middle panel of Fig. 2 the peak position is shown vs time for the 9 LRPD and 4 WT observations, respectively. Errors are relative to 90% confidence level. In the bottom panel the Crab profile for the longest contemporaneous RXTE observations is shown.

Fitting the RXTE results we get a lag with respect to the radio peak of  $396 \pm 200 \mu\text{s}$  well in agreement with the results quoted by<sup>12</sup> ( $344 \pm 40 \mu\text{s}$ ).

Averaging the phases of the first peak maximum in the 9 LRPD and in the 4 WT observations we have a phase position of the X-ray peak of  $0.990 \pm 0.006$ , and  $0.988 \pm 0.010$  corresponding to a lag with respect to the radio pulse of  $335 \pm 200 \mu\text{s}$  and  $403 \pm 300 \mu\text{s}$ , respectively. The quoted errors are the rms with respect to the

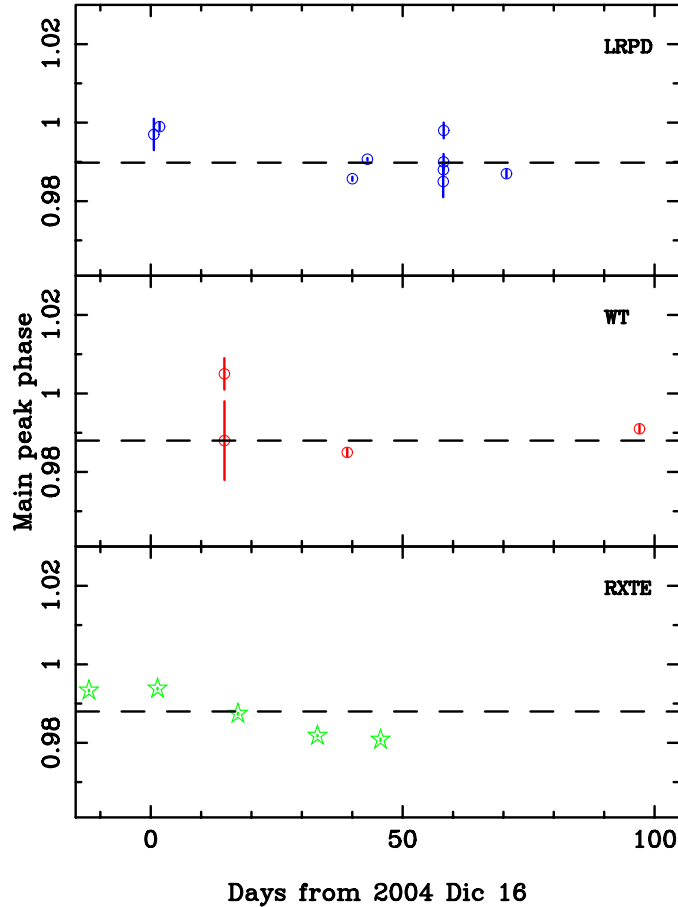


**Figure 2.** The phases of the main peak relative to 9 LRPD and 4 WT observations vs time are plotted in the top and middle panel, respectively. The bottom panel shows, for comparison, the values relative to the contemporaneous RXTE observations. The dashed lines represents the average values.

means and are representative of the systematics in the XRT absolute time capability.

#### 4. CONCLUSION

We analyzed observations of the Crab pulsar performed over a 3 month time interval by Swift-XRT in LRPD and WT mode. All observations show a Crab profile with the correct shape. The average values of the main peak phase positions are well in agreement with the results obtained from the contemporaneous RXTE observations. Moreover, the absolute phase has been reconstructed with a time accuracy of  $200 \mu\text{s}$  and  $300 \mu\text{s}$  for the LRPD and WT observation mode, respectively. The time precision has been evaluated through the rms of the main peak absolute phase measured respect to the mean.

#### ACKNOWLEDGMENTS

This work is supported at OAB by ASI grant I/R/039/04, at Penn State by NASA contract NAS5-00136 and at the University of Leicester by PPARC of grants PPA/G/S/00524 and PPA/Z/S/2003/00507. We gratefully acknowledge the contributions of dozens of members of the XRT and UVOT team at OAB, PSU, UL, GSFC, ASDC, and MSSL and our subcontractors, who helped make this instrument possible.

## REFERENCES

1. N.Gehrels, G.Chincarini, P.Giommi, and et al., "The swift gamma-ray burst mission," *ApJ* **611**, p. 1005, 2004.
2. S. Barthelmy and et al., "Burst alert telescope (bat) on the swift midex mission," *Sp.Sc.Rev.*, **120**, 2005.
3. D. Burrows, J.E.Hill, J.A.Nousek, and et al., "The swift x-ray telescope," *Sp.Sc.Rev.* **120**, 2005.
4. P. Roming and et al., "The swift ultra-violet/optical telescope," *Sp.Sc.Rev.* **120**, 2005.
5. O.Citterio, S.Campana, P.Conconi, and et al., "Characteristics of the flight model optics for the jet-x telescope onboard the spectrum-x-gamma satellite," *SPIE* **2805**, p. 56, 1996.
6. A.A.Wells, C.C.Castelli, M.Denby, and et al., "X-ray imaging performance of the flight model jet-x telescope," *SPIE* **3134**, p. 392, 1997.
7. A.D.Holland, M.J.Turner, A.F.Abbey, and P.J.Pool, "Mos ccds for the epic on xmm," *SPIE* **2808**, p. 41, 1996.
8. A.Moretti and et al., "The swift xrt point spread function,," *SPIE this volume*, 2005.
9. P.Romano and et al., "In-flight calibration of the swift xrt effective area,," *SPIE this volume*, 2005.
10. J.E.Hill, R.Klar, C.Chervu, R.M.Ambrosi, and D.N.Burrows, "Readout modes and automated operation of the swift x-ray telescope," *SPIE* **5165**, p. 217, 2004.
11. K.Jahoda, J.H.Swank, A.B.Giles, and M.J.Stark, "In-orbit performance and calibration of the rossi x-ray timing explorer (rxte) proportional counter array (pca)," *SPIE* **2808**, p. 59, 1996.
12. A.H.Rots, K.Jahoda, and A. Lyne, "Absolute timing of the crab pulsar with the rossi x-ray timing explorer," *ApJ* **605**, p. 129, 2004.